J. Appl. Comput. Mech., 5(5) (2019) 827-839
DOI: 10.22055/JACM.2019.27677.1428

ISSN: 2383-4536
jacm.scu.ac.ir

M&MoCS

Shahid Chamran University of Ahvaz

Journal of Applied and Computational Mechanics

Research Paper

An Analytical and Semi-analytical Study of the Oscillating Flow of Generalized Burgers' Fluid through a Circular Porous Medium

Abdul Rauf

Department of Computer Science & Engineering, Air University,
Abdali Road, Khan Center, Multan, 60000, Pakistan, abdul.rauf@aumc.edu.pk

Received November 26 2018; Revised February 21 2019; Accepted for publication February 26 2019.
Corresponding author: Abdul Rauf, abdul.rauf@aumc.edu.pk

Abstract. Unsteady oscillatory flow of generalized Burgers' fluid in a circular channel tube in the porous medium is investigated under the influence of time-dependent trapezoidal pressure gradient given by an infinite Fourier series. An exact analytical expression for the solution for the fluid velocity and the shear stress are recovered by using the similarity arguments together with the integral transforms. The solution is verified with a semi-analytical solution obtained by employing the Stehfest's method. Using the software Mathcad, numerical calculations have been carried out, and results are presented in graphical illustrations in order to analyze the effects of various fluid parameters on the fluid motion. As expected, with the increase in the permeability of the porous medium, the drag force decreases, which results in an increase in the velocity profile for all kinds of fluid models (a generalized Burgers' fluid, a Burgers' fluid, a Maxwell fluid, and an Oldroyd-B fluid). Moreover, it has been observed that the material constants of the generalized Burgers' fluid, as well as the Burgers' fluid, are other important factors that enhance the flow velocity performance of the fluid. The velocity-time variation for the generalized Burgers' fluid, the Oldroyd-B fluid, and the Newtonian fluid is similar to the trapezoidal waveform, whereas it is different for the Burgers' and Maxwell fluid.

Keywords: Oscillating motion, Porous medium, Trapezoidal pressure gradient, Generalized Burgers' fluid, Analytical and semi-analytical solution.

1. Introduction

In the modern era, viscoelastic fluids have wide research interest due to their many useful applications. For example, viscoelastic fluids occur in the exotic lubricants, extrusion of polymer fluids, cooling of a metallic plate in a bath, colloidal and suspension solutions and artificial and natural gels. Such flows become more important in porous media due to their applications in engineering. Typical applications include paper and textile coating, enhanced oil recovery, and composite manufacturing processes. A good amount of work in the theory of viscoelastic flows with a fractional calculus approach [1-6] is done in the literature. This is natural for the description of complex dynamical systems such as polymeric materials. The complexity and unpredictability in the configurational dynamics of such polymeric materials are a result of polymer chain configurations. This is reflected in the discontinuity in the chain segment movements and in the propensity for the particles to the group and in this way move collectively.

The investigation of the flow through a permeable porous medium is of major significance in industry, bio and geomechanics, e.g. liquids filtration and flow of water from mountains and stones. The solid matrix having bores in it forms the porous medium. Permeability and porosity are the two main characters of porous media. Prior investigations reveal that it can be described by Darcy's law. The study of fluid flow through a porous medium is an important and hot topic due to its several applications. For example, this study helps in the suction of unrefined petroleum from the pores of the stones. In [7],

Published online: May 17 2019

Jyothi et al. considered the cylindrical surface with inside having porous medium linings and contemplated the pulsatile flow of Jeffrey fluid. The unsteady non-Newtonian fluid flow due to rectified sinusoidal pulses is studied in [8]. In [9], Elshehawey et al. examined the peristaltic transport in a porous medium through an asymmetric channel .

Numerous scientists and researchers have contemplated the unsteady non-Newtonian fluids flow under the influence of the oscillating pressure gradient [10-16]. For instance, in [17] Manos et al. presented the exact analytical solution for the Jeffrey fluid flows in the curved duct caused by an oscillating circumferential pressure gradient. The results are verified numerically with the finite difference method. Exact analytical solutions for the motion of fraction Burgers' fluid driven by infinite plan oscillation as well as by the application of oscillating pressure gradient is investigated by the Khan et al. [18]. They used an integral transform (Laplace and Fourier transform) methods to solve the partial differential equations governing the problem. In [19], authors studied the generalized Maxwell fluid rotating flow in annulus region between two circular cylinders. The flow is caused by the time-dependent oscillating and rotating pressure gradient applied to the inner cylinder. The integral transforms, Laplace and Hankel are used for the solution.

Above discussion shows that a lot of work has been done to investigate the flow with a sinusoidal waveform effect on an oscillating flow but the study of oscillating flow with trapezoidal pressure waveform is a lack in literature. In [20], Ruckmongathan has observed that the triangular and trapezoidal waveforms are helpful to minimize the power consumption in liquid crystal displays in electronics. This provides a motivation to study the unanswered problems corresponding to fluid flow caused by the trapezoidal pressure waveforms.

To the best of my knowledge, an oscillating flow under the effect of trapezoidal pressure waveform for generalized Burgers' fluid in a porous medium is yet to be investigated. We considered this problem in this paper and obtained analytical and semi-analytical solutions for velocity distribution profile. We used finite Hankel transform and similarity arguments to recover analytical solution. The solution is verified numerically with Stehfests' algorithm used for numerical inversion of Laplace transform.

2. Mathematical Modeling of the Problem

The constitutive equations for generalized Burgers' fluids are given by [21]

$$\mathcal{T}=\mathcal{S}-p\mathbf{I},\ \lambda_2\frac{\delta^2\mathcal{S}}{\delta t^2}+\lambda_1\frac{\delta\mathcal{S}}{\delta t}+\mathcal{S}=\mu\left[\lambda_4\frac{\delta^2\mathbf{A}}{\delta t^2}+\lambda_3\frac{\delta\mathbf{A}}{\delta t}+\mathbf{A}\right] \tag{1}$$

where $\mathcal{T}$ is the Cauchy stress tensor $-p\mathbf{I}$ is the indeterminate spherical stress, $\mathcal{S}$ is the extra stress tensor, $\mathbf{A}=\mathbf{L}^T+\mathbf{L},\ \mathbf{L}=\nabla\mathbf{v}$, μ is the dynamic viscosity of the fluid, $\lambda_1,\ \lambda_3$ are the relaxation time and retardation time respectively, $\lambda_2,\ \lambda_4$ are the material parameters heaving the dimension $[s^2]$ and $\delta/\delta t$ denotes the upper convected derivative defined as

$$\frac{\delta^2\mathcal{S}}{\delta t^2}=\frac{\delta}{\delta t}\left(\frac{\delta\mathcal{S}}{\delta t}\right)=\frac{\delta}{\delta t}\left((\frac{d}{dt}-\mathbf{L})\mathcal{S}-\mathcal{S}\mathbf{L}^T\right). \tag{2}$$

The generalized Burgers' model given by Eq. (1) reduces at Burgers' fluid for $\lambda_4=0$, Oldroyd-B fluid for $\lambda_2=\lambda_4=0$, Maxwell fluid for $\lambda_2=\lambda_3=\lambda_4=0$ and the Newtonian fluid for $\lambda_1=\lambda_2=\lambda_3=\lambda_4=0$. Assume a capillary tube of radius R with an axis of rotation along the z-axis. The capillary tube is filled with an incompressible, homogeneous, laminar and viscoelastic Burgers' fluid (Fig. 1). The capillary tube is driven by the applied pressure gradient in the axial direction that varies with trapezoidal pressure form, that is

$$-\nabla p=P_0(8+f(t))\mathbf{e}_z,P_0\neq 0, \tag{3}$$

where

$$f(t)=\frac{P_1}{P_0}\sum_{l=0}^{\infty}g_{trp}\left(t-2l\pi\right)=\frac{P_1}{P_0}\sum_{k=1}^{\infty}a_k sin(kt), \tag{4}$$

$$g_{trp}(t)=\begin{cases}-4-\dfrac{4t}{\pi}, & -\pi\le t\le-\dfrac{3\pi}{4}\\ -1, & -\dfrac{3\pi}{4}\le t\le-\dfrac{\pi}{4}\\ \dfrac{4t}{\pi}, & -\dfrac{\pi}{4}\le t\le\dfrac{\pi}{4}\\ 1, & \dfrac{\pi}{4}\le t\le\dfrac{3\pi}{4}\\ 4-\dfrac{4t}{\pi}, & \dfrac{3\pi}{4}\le t\le\pi\end{cases}, \tag{5}$$

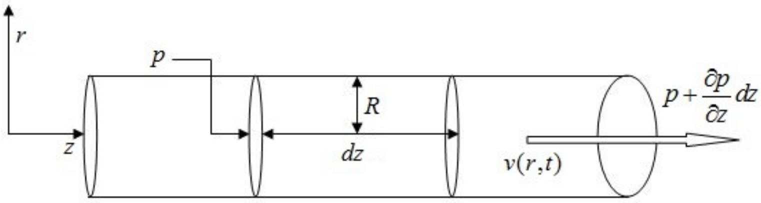

Fig. 1. Geometry of the problem

$$a_k = \frac{8}{\pi^2 k^2}\left[\sin\left(\frac{3\pi k}{4}\right)+\sin\left(\frac{k\pi}{4}\right)\right], \tag{6}$$

in which $\mathbf{e}_z$ is the unit vector in the z -direction parallel to the direction of the flow and P_0, P_1 are the amplitudes for the steady and pulsating part of the pressure gradient in the axial direction. We assume that the fluid velocity $\mathbf{v}$ and the extra stress tensor $\mathcal{S}$ are of the form

$$\mathbf{v}=\mathbf{v}(r,t)=v(r,t)\mathbf{e}_z,\ \mathcal{S}=\mathcal{S}(r,t)=\mathcal{S}(r,t)\mathbf{e}_z. \tag{7}$$

Introducing Eqs. (7) and $\mathcal{S}(r,0)=0$ in (1), we get [22]

$$\tau_{rz}+\lambda_1\frac{\partial \tau_{rz}}{\partial t}+\lambda_2\frac{\partial^2\tau_{rz}}{\partial t^2}=\mu(\lambda_4\frac{\partial^2}{\partial t^2}+\lambda_3\frac{\partial}{\partial t}+1)\frac{\partial v}{\partial r}, \tag{8}$$

where $\tau_{rz}=\mathcal{S}_{rz}(r,t)$ is one of the nonzero component of the extra stress tensor. The continuity equation and the balance of linear momentum in the absence of body force for the incompressible porous medium are

$$\nabla\cdot\mathbf{v}=0, \tag{9}$$

$$\rho(\mathbf{v}.\nabla\mathbf{v}+\frac{\partial \mathbf{v}}{\partial t})=-\nabla p+\nabla\cdot\mathcal{S}+\mathcal{R}_d, \tag{10}$$

where ρ is density, p is pressure and $\mathcal{R}_d$ is Darcy's resistance of porous medium. The Darcy's resistance for generalized Burgers' fluid is given by the following equation [23]

$$\left(1+\lambda_1\frac{\partial}{\partial t}+\lambda_2\frac{\partial^2}{\partial t^2}\right)\mathcal{R}_d=-\frac{\mu\psi}{k_0}\left(1+\lambda_3\frac{\partial}{\partial t}+\lambda_4\frac{\partial^2}{\partial t^2}\right)\mathbf{v}, \tag{11}$$

where $\mathcal{R}_d=\mathcal{R}\mathbf{e}_z$, k_0 is the permeability constant of the medium and ψ is the porosity of the medium. In the presence of pressure gradient (3), the balance of linear momentum Eq. (10) takes the form

$$\rho\frac{\partial v}{\partial t}=P_0(8+f(t))+\frac{1}{r}\frac{\partial}{\partial r}(r\tau_{rz})+\Re, \tag{12}$$

where τ_{rz} is shear stress in the axial direction. Applying the operator $(1+\lambda_1[\partial/\partial t]+\lambda_2[\partial^2/\partial t^2])$ to Eq. (12) and using Eqs. (3), (8) and (11) we get

$$\begin{aligned}\rho\left(1+\lambda_1\frac{\partial}{\partial t}+\lambda_2\frac{\partial^2}{\partial t^2}\right)\frac{\partial v}{\partial t}-P_0\left(1+\lambda_1\frac{\partial}{\partial t}+\lambda_2\frac{\partial^2}{\partial t^2}\right)(8+f(t))\\ =\mu(\lambda_4\frac{\partial^2}{\partial t^2}+\lambda_3\frac{\partial}{\partial t}+1)\frac{1}{r}\frac{\partial}{\partial r}(r\frac{\partial v}{\partial r})-\frac{\mu\psi}{k_0}\left(1+\lambda_3\frac{\partial}{\partial t}+\lambda_4\frac{\partial^2}{\partial t^2}\right)v.\end{aligned} \tag{13}$$

The appropriate boundary conditions for velocity are

$$v(R,t)=0,\ \frac{\partial v(r,t)}{\partial r}|_{r=0}=0. \tag{14}$$

We introduce the following dimensionless parameters in Eqs. (13) and (14),

$$v^*=\frac{v}{v_m},t^*=\frac{\nu t}{R^2},v_m=\frac{P_0R^2}{\mu},r^*=\frac{r}{R},\omega=\frac{R^2}{\nu},\lambda_1^*=\frac{\lambda_1}{\omega},\ \lambda_2^*=\frac{\lambda_2}{\omega^2},\lambda_3^*=\frac{\lambda_3}{\omega},\lambda_4^*=\frac{\lambda_4}{\omega^2},f^*(t^*)=f(\omega t^*),\frac{1}{K_0}=\frac{\psi R^2}{k_0}. \tag{15}$$

where K_0 is the permeability parameter of the porous medium. Dropping the "*" notations, the governing Eq. (13) in non-dimensional form

$$\left(\lambda_2 \frac{\partial^2}{\partial t^2}+\lambda_1 \frac{\partial}{\partial t}+1\right)\frac{\partial v}{\partial t}-\left(\lambda_2 \frac{\partial^2}{\partial t^2}+\lambda_1 \frac{\partial}{\partial t}+1\right)(8+f(t))=(\lambda_4 \frac{\partial^2}{\partial t^2}+\lambda_3 \frac{\partial}{\partial t}+1)\frac{1}{r}\frac{\partial}{\partial r}(r\frac{\partial v}{\partial r})-\frac{1}{K_0}\left(1+\lambda_3 \frac{\partial}{\partial t}+\lambda_4 \frac{\partial^2}{\partial t^2}\right)v, \tag{16}$$

along with the boundary conditions (14)

$$v(1,t)=0,\ \frac{\partial v(r,t)}{\partial r}\Big|_{r=0}=0. \tag{17}$$

The trapezoidal harmonics is

$$f(t)=P\sum_{k=1}^{\infty} a_k \sin(k\omega t), \tag{18}$$

where $P=P_1/P_0$.

3. Solution of the Problem

3.1 Steady state solution

We assume that the solution of Eq. (16) is of the form

$$v(r,t)=v_s(r)+v_t(r,t) \tag{19}$$

where $v_s(r)$ is the steady state solution and $v_t(r,t)$ is the transient part of the solution. The property of this solution is that when $t\to\infty$, we recover the steady part of the solution. Substituting the Eq. (19) in Eq. (16), we obtain

$$\frac{\partial^2 v_s}{\partial r^2}+\frac{1}{r}\frac{\partial v_s}{\partial r}-\frac{v_s}{K_0}=-8, \tag{20}$$

$$\begin{aligned}&\left(\lambda_2 \frac{\partial^2}{\partial t^2}+\lambda_1 \frac{\partial}{\partial t}+1\right)\frac{\partial v_t}{\partial t}-\left(\lambda_2 \frac{\partial^2}{\partial t^2}+\lambda_1 \frac{\partial}{\partial t}+1\right)f(t)\\ &=\left(\lambda_4 \frac{\partial^2}{\partial t^2}+\lambda_3 \frac{\partial}{\partial t}+1\right)\left(\frac{\partial^2 v_t}{\partial r^2}+\frac{1}{r}\frac{\partial v_t}{\partial r}\right)-\frac{1}{K_0}\left(\lambda_4 \frac{\partial^2}{\partial t^2}+\lambda_3 \frac{\partial}{\partial t}+1\right)v_t.\end{aligned} \tag{21}$$

The general solution for non-homogeneous Eq. (20) can be found as the sum of a solution for homogeneous part with a particular solution. The homogeneous part of Eq. (20) is

$$x^2\frac{\partial^2 v_s}{\partial x^2}+x\frac{\partial v_s}{\partial x}+x^2 v_s=0, \tag{22}$$

where we substituted $x=\iota r\sqrt{K_0^{-1}}$ and $\iota=\sqrt{-1}$. Eq. (22) is the Bessel differential equation of order zero with the solution

$$v_{sh}(r)=c_1 I_0\left(r\sqrt{K_0^{-1}}\right)+c_2 Y_0\left(-\iota r\sqrt{K_0^{-1}}\right), \tag{23}$$

where we replaced back $x=\iota r\sqrt{K_0^{-1}}$, I_0 is the modified Bessel function of the first kind of order zero, Y_0 is the Bessel function of the second kind of order zero. It is trivial to see that the particular solution of Eq. (20) is

$$v_{sp}=8K_0. \tag{24}$$

The general solution for nonhomogeneous Eq. (20) is

$$v_s(r)=c_1 I_0\left(r\sqrt{K_0^{-1}}\right)+c_2 Y_0\left(-\iota r\sqrt{K_0^{-1}}\right)+8K_0. \tag{25}$$

With the help of boundary conditions (17), we find that $c_1=-8K_0/(I_0(\sqrt{K_0^{-1}}))$, $c_2=0$, thus the steady state solution for the velocity is

$$v_s(r)=-\frac{8K_0}{I_0\left(\sqrt{K_0^{-1}}\right)}I_0\left(r\sqrt{K_0^{-1}}\right)+8K_0. \tag{26}$$

3.2 Transient solution

In order to find the transient velocity of the fluid we apply the finite Hankel transform to Eq. (21)

$$\begin{aligned}&\left(\lambda_2\frac{\partial^2}{\partial t^2}+\lambda_1\frac{\partial}{\partial t}+1\right)\frac{\partial v_t(r_n,t)}{\partial t}-\frac{J_1(r_n)}{r_n}\left(\lambda_2\frac{\partial^2}{\partial t^2}+\lambda_1\frac{\partial}{\partial t}+1\right)f(t)\\&=\left(\lambda_4\frac{\partial^2}{\partial t^2}+\lambda_3\frac{\partial}{\partial t}+1\right)\left(-r_n^2v_t(r_n,t)\right)-\frac{1}{K_0}\left(\lambda_4\frac{\partial^2}{\partial t^2}+\lambda_3\frac{\partial}{\partial t}+1\right)v_t(r_n,t),\end{aligned} \tag{27}$$

where $v_t(r_n,t)=\int_0^1 rv_t(r,t)J_0(r_nr)dr$, J_0 is the zeroth order Bessel function of first kind and $J_0(r_n)=0$ for all n. Consider that the solution of Eq. (27) is in the series form

$$v_t(r_n,t)=\sum_{k=1}^{\infty}\left[a_{nk}\cos(k\omega t)+b_{nk}\sin(k\omega t)\right]. \tag{28}$$

where a_{nk}, b_{nk} are coefficients to be determined. Substituting Eqs. (18) and (28) in Eq. (27) and comparing the coefficients of $\sin(k\omega t)$ and $\cos(k\omega t)$ respectively, we have the following system of equations,

$$\alpha_{nk}a_{nk}-\beta_{nk}b_{nk}=Pa_k(-1+\lambda_2(k\omega)^2)\frac{J_1(r_n)}{r_n},\; n,k=1,2,3,\ldots, \tag{29}$$

$$\beta_{nk}a_{nk}+\alpha_{nk}b_{nk}=P\lambda_1k\omega a_k\frac{J_1(r_n)}{r_n},\; n,k=1,2,3,\ldots, \tag{30}$$

where

$$\alpha_{nk}=-\lambda_2(k\omega)^3+(1+r_n^2\lambda_3+\frac{\lambda_3}{K_0})k\omega,\; n,k=1,2,3,\ldots, \tag{31}$$

$$\beta_{nk}=r_n^2+\frac{1}{K_0}-(\lambda_1+\lambda_4r_n^2+\frac{\lambda_4}{K_0})(k\omega)^2,\; n,k=1,2,3,\ldots. \tag{32}$$

Solving the system of Eqs. (29) and (30) we get

$$a_{nk}=Pa_k\varepsilon_{nk}\frac{J_1(r_n)}{r_n},\; n,k=1,2,3,\ldots, \tag{33}$$

$$b_{nk}=Pa_k\delta_{nk}\frac{J_1(r_n)}{r_n},\; n,k=1,2,3,\ldots, \tag{34}$$

where

$$\varepsilon_{nk}=\frac{[\lambda_2(k\omega)^2-1]\alpha_{nk}+\lambda_1k\omega\beta_{nk}}{\alpha_{nk}^2+\beta_{nk}^2}, \tag{35}$$

$$\delta_{nk}=\frac{\lambda_1k\omega\alpha_{nk}-[\lambda_2(k\omega)^2-1]\beta_{nk}}{\alpha_{nk}^2+\beta_{nk}^2}. \tag{36}$$

With the help of Eqs (33)-(36), the solution of differential equation (27) in the series form takes the form,

$$v_t(r_n,t)=P\frac{J_1(r_n)}{r_n}\sum_{k=1}^{\infty}a_k[\varepsilon_{nk}\cos(k\omega t)+\delta_{nk}\sin(k\omega t)]. \tag{37}$$

If $v(r,t)$, $r\in[0,1]$ has the Hankel transform $v(r_n,t)$, the inverse Hankel is

$$v(r,t)=2\sum_{n=1}^{\infty}\frac{J_0(rr_n)}{J_1^2(r_n)}v(r_n,t). \tag{38}$$

The transient part of the velocity can be obtained by applying the inverse Hankel transform to Eq. (37)

$$v_t(r,t) = 2P\sum_{n=1}^{\infty}\left\{\frac{J_0(rr_n)}{r_n J_1(r_n)}\sum_{k=1}^{\infty} a_k\left[\varepsilon_{nk}\cos(k\omega t)+\delta_{nk}\sin(k\omega t)\right]\right\}. \tag{39}$$

The solution for velocity field can be obtained by inserting Eqs. (26), (39) in Eq. (19),

$$v(r,t) = -\frac{8K_0}{I_0\left(\sqrt{K_0^{-1}}\right)} I_0\left(r\sqrt{K_0^{-1}}\right) + 8K_0 + 2P\sum_{n=1}^{\infty}\left\{\frac{J_0(rr_n)}{r_n J_1(r_n)}\sum_{k=1}^{\infty} a_k\left[\varepsilon_{nk}\cos(k\omega t)+\delta_{nk}\sin(k\omega t)\right]\right\} \tag{40}$$

3.3 Semi-analytical Solution

In this section, we determine a new form of solutions to the problem given by Eqs. (16) and using the Laplace transform coupled with the classical method for the ordinary differential equations. For a comparative study of solutions, we used the following initial conditions to solve Eq. (27),

$$v_t(r,0) = g_0(r), \frac{\partial v_t(r,0)}{\partial t} = g_1(r), \frac{\partial^2 v_t(r,0)}{\partial t^2} = g_2(r). \tag{41}$$

where g_0, g_1 and g_2 are piece-wise continuous functions. The finite Hankel transform $\mathcal{H}_n$ form of initial conditions in Eq. (41) is

$$\mathcal{H}_n\{v_t(r,0)\} = \mathcal{H}_n\{g_0(r)\} = \gamma_{0n},\ \mathcal{H}_n\left\{\frac{\partial v_t(r,0)}{\partial t}\right\} = \mathcal{H}_n\{g_1(r)\} = \gamma_{1n},\ \mathcal{H}_n\left\{\frac{\partial^2 v_t(r,0)}{\partial t^2}\right\} = \mathcal{H}_n\{g_2(r)\} = \gamma_{2n}. \tag{42}$$

Applying the Laplace transform to Eq. (27) along with the initial conditions (42) we get the transformed transient velocity in the form

$$\bar{v}_t(r_n,q) = \mathcal{A}(r_n,q) + \mathcal{B}(r_n,q)\frac{J_1(r_n)}{r_n}, \tag{43}$$

where

$$\mathcal{A}(r_n,q) = \frac{\gamma_{0n}\{1+\lambda_3(r_n^2+K_0^{-1})+[\lambda_1+\lambda_4(r_n^2+K_0^{-1})]q+\lambda_2 q^2\}+\gamma_{1n}[\lambda_1+\lambda_2 q-\lambda_4(r_n^2+K_0^{-1})]+\gamma_{2n}\lambda_2}{\lambda_2 q^3+[\lambda_1+\lambda_4(r_n^2+K_0^{-1})]q^2+[1+\lambda_3(r_n^2+K_0^{-1})]q+(r_n^2+K_0^{-1})} \tag{44}$$

$$\mathcal{B}(r_n,q) = P\sum_{k=1}^{\infty}\frac{k\omega a_k(1-\lambda_2 k^2\omega^2+\lambda_1 q)}{\{\lambda_2 q^3+[\lambda_1+\lambda_4(r_n^2+K_0^{-1})]q^2+[1+\lambda_3(r_n^2+K_0^{-1})]q+(r_n^2+K_0^{-1})\}(q^2+k^2\omega^2)} \tag{45}$$

Here we have used $\bar{f}(q) = P\sum_{k=1}^{\infty} a_k\frac{k\omega}{q^2+k^2\omega^2}$, $f'(0) = P\sum_{k=1}^{\infty} a_k k\omega$, and $\bar{v}_t(r_n,q) = \int_0^{\infty} v_t(r_n,t)e^{-qt}dt$ is the Laplace transform of $v_t(r_n,q)$. By applying the inverse Hankel transform to Eq. (43)

$$\bar{v}_t(r,q) = 2\sum_{n=1}^{\infty}\frac{J_0(rr_n)}{J_1^2(r_n)}\mathcal{A}(r_n,q) + 2\sum_{n=1}^{\infty}\frac{J_0(rr_n)}{r_n J_1(r_n)}\mathcal{B}(r_n,q), \tag{46}$$

In order to obtain the inverse Laplace transform, we use an accuracy numerical algorithm, namely the Stehfest's algorithm [24, 25] for numerical Laplace transform inversion

$$v_t(r,t) = \frac{\ln 2}{t}\sum_{i=1}^{M} L_i \bar{v}_t\left(r, i\frac{\ln 2}{t}\right) \tag{47}$$

$$L_i = (-1)^{i+M/2}\sum_{K=(i+1)/2}^{\min(i,M/2)}\frac{K^{M/2}(2K)!}{(M/2-K)!(i-K)!(2K-i)!K!}, \tag{48}$$

where a free integral parameter M represents the number of terms used in the summation of Eq. (47).

3.4 Derivations of the shear stress

Applying the differential operator $\mu(\lambda_4\partial^2/\partial t^2+\lambda_3\partial/\partial t+1)\times\partial/\partial r$ to Eq. (40) and using Eq. (8), we get

$$\tau_{rz}+\lambda_1\frac{\partial\tau_{rz}}{\partial t}+\lambda_2\frac{\partial^2\tau_{rz}}{\partial t^2}=-2\mu P\sum_{n=1}^{\infty}\Big[\frac{J_1(rr_n)}{J_1(r_n)}\sum_{k=1}^{\infty}a_k\big(\alpha_{nk}\cos(k\omega t)+\beta_{nk}\sin(k\omega t)\big)\Big],\tag{49}$$

where $\alpha_{nk}=-\lambda_4k^2\omega^2\varepsilon_{nk}+\lambda_3k\omega\delta_{nk}+\varepsilon_{nk}$, $\beta_{nk}=-\lambda_4k^2\omega^2\delta_{nk}-\lambda_3k\omega\varepsilon_{nk}+\delta_{nk}$. Applying the Laplace transform along with the initial conditions $\tau_{rz}(r,0)=\partial\tau_{rz}(r,t)/\partial t|_{t=0}=0,$ we can write

$$\bar{\tau}_{rz}(r,q)=-2\mu P\sum_{n=1}^{\infty}\Big[\frac{J_1(rr_n)}{J_1(r_n)}\sum_{k=1}^{\infty}a_k\Big(\frac{\alpha_{nk}q}{(q^2+k^2\omega^2)(1+\lambda_1q+\lambda_2q^2)}+\frac{k\omega\beta_{nk}}{(q^2+k^2\omega^2)(1+\lambda_1q+\lambda_2q^2)}\Big)\Big].\tag{50}$$

Applying the inverse Laplace transform to Eq. (50), we recover the shear stress $\tau_{rz}(r,t)$,

$$\tau_{rz}(r,t)=-2\mu P\sum_{n=1}^{\infty}\Big[\frac{J_1(rr_n)}{J_1(r_n)}\sum_{k=1}^{\infty}a_k\big(\alpha_{nk}F_{1k}(t)+\beta_{nk}F_{2k}(t)\big)\Big],\tag{51}$$

where

$$\begin{aligned}F_{1k}(t)=&\frac{e^{\frac{-(\lambda_1+\sqrt{-4\lambda_2+\lambda_1^2})t}{2\lambda_2}}\Big(-\lambda_1(1+\lambda_2k^2\omega^2)(-1+e^{\frac{\sqrt{-4\lambda_2+\lambda_1^2}t}{\lambda_2}})+\sqrt{-4\lambda_2+\lambda_1^2}(-1+\lambda_2k^2\omega^2)(-1+e^{\frac{\sqrt{-4\lambda_2+\lambda_1^2}t}{\lambda_2}})\Big)}{2\sqrt{-4\lambda_2+\lambda_1^2}(1+k^2\omega^2(\lambda_1^2+\lambda_2(-2+\lambda_2k^2\omega^2)))}\\&-\frac{2\sqrt{-4\lambda_2+\lambda_1^2}e^{\frac{(\lambda_1+\sqrt{-4\lambda_2+\lambda_1^2})t}{2\lambda_2}}((-1+\lambda_2k^2\omega^2)\cos(k\omega t)-\lambda_1k\omega\sin(k\omega t))}{2\sqrt{-4\lambda_2+\lambda_1^2}(1+k^2\omega^2(\lambda_1^2+\lambda_2(-2+\lambda_2k^2\omega^2)))},\end{aligned}\tag{52}$$

$$\begin{aligned}F_{2k}(t)=&\frac{\lambda_1k\omega e^{\frac{(-\lambda_1+\sqrt{-4\lambda_2+\lambda_1^2})t}{2\lambda_2}}+\lambda_1k\omega e^{-\frac{(\lambda_1+\sqrt{-4\lambda_2+\lambda_1^2})t}{(2\lambda_2)}}+2\sin(k\omega t)-2k\omega(\lambda_1\cos(k\omega t)+\lambda_2k\omega\sin(k\omega t))}{2(1+k^2\omega^2(\lambda_1^2+\lambda_2(-2+\lambda_2k^2\omega^2)))}\\&+\frac{k\omega(\lambda_1^2+2\lambda_2(-1+\lambda_2k^2\omega^2))e^{-\frac{((\lambda_1+\sqrt{-4\lambda_2+\lambda_1^2})t}{2\lambda_2}}(-1+e^{\frac{\sqrt{-4\lambda_2+\lambda_1^2}t}{\lambda_2}})}{2\sqrt{-4\lambda_2+\lambda_1^2}(1+k^2\omega^2(\lambda_1^2+\lambda_2(-2+\lambda_2k^2\omega^2)))}.\end{aligned}\tag{53}$$

4. Numerical Results and Discussions

In the sections 3, analytical and semi-analytical results for the flow problem of a generalized Burgers' fluid model are recovered. The motion of fluids is generated by the channel tube, which is moving with the time-dependent velocities, and by the time-dependent trapezoidal pressure gradient in the flow direction.

Closed form for the fluid velocity has been determined by coupling the finite Hankel transform with the series solution. The semi-analytical solution for the velocity field has been obtained by employing the Laplace transform and Stehfest's algorithms for the numerical inversion of the Laplace transform. The obtained results have a general character; therefore, many particular cases such as Burgers' fluid, Oldroyd-B fluid, Maxwell fluid, and Newtonian fluid can be obtained.

Using the software Mathcad, numerical calculations were carried out for the obtained solutions. Numerical results are presented in Figs. 2-11 and Table 1. The influence of the trapezoidal waveform, the permeability of porous medium and material parameters on the time-dependent flow is studied graphically.

Fig. 2 and table 1 provides a comparative study of the numerical and analytical transient velocity $v_t(r,t)$ of the generalized Burgers' fluid. It can be seen that the performance of the numerical transient velocity (47) correlates with the analytical transient velocity (39). Fig. 2 depicts that a good agreement between both analytical and numerical solutions of the transient velocity $v_t(r,t)$ is observed. Table 1 depicts that the error between analytical and numerical solutions of the transient velocity $v_t(r,t)$ is up to order 10^{-8} and therefore is negligible.

We prepared the Figs. 3-6 to demonstrate the influence of permeability of porous medium K_0 on the fluid velocity for various types of fluid models. These include a generalized Burgers' fluids for which $\lambda_4=1.5,\lambda_3=0.76,\lambda_2=5,\lambda_1=9,$ a Burgers' fluid for which $\lambda_4=0,\lambda_3=0.76,\lambda_2=5,\lambda_1=9,$ an Oldroyd-B fluid for which $\lambda_4=0,\lambda_3=0.76,\lambda_2=0,\lambda_1=9$, and a Maxwell fluid for which $\lambda_4=0,\lambda_3=0,\lambda_2=0,\lambda_1=9.$

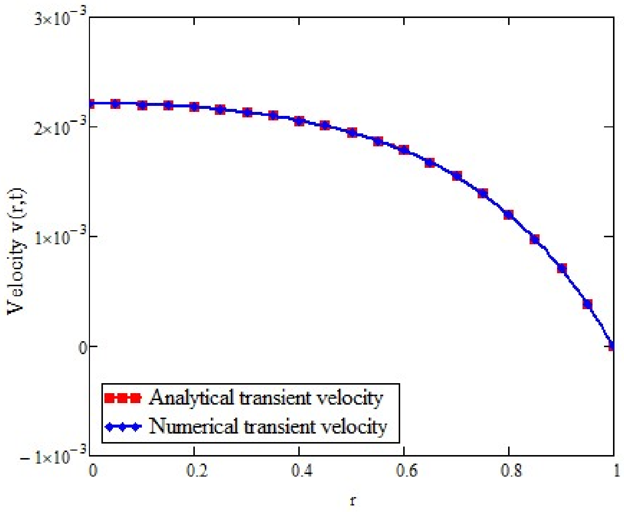

Fig. 2. Comparison of the numerical and analytical transient velocity $v_t(r,t)$ for $t=0.5, \omega=0.26, K_0=0.1,\ \lambda_1=0.37,\ \lambda_2=0.43, \lambda_3=0.59$

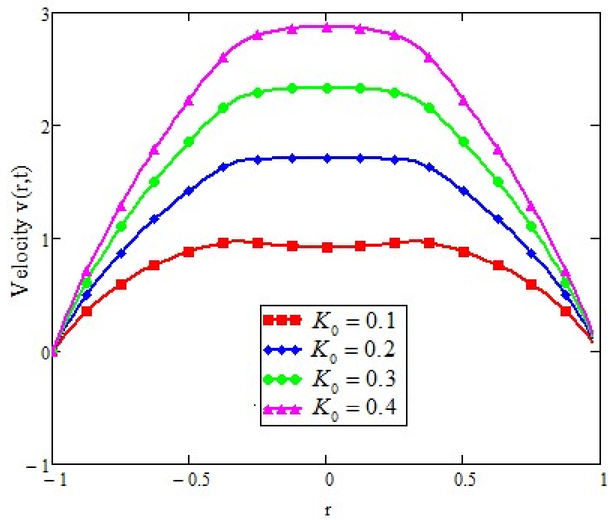

Fig. 3. Velocity profile $v(r,t)$ versus r for Maxwell fluid for $t=1$, $\omega=\pi/4$ and for different values of K_0.

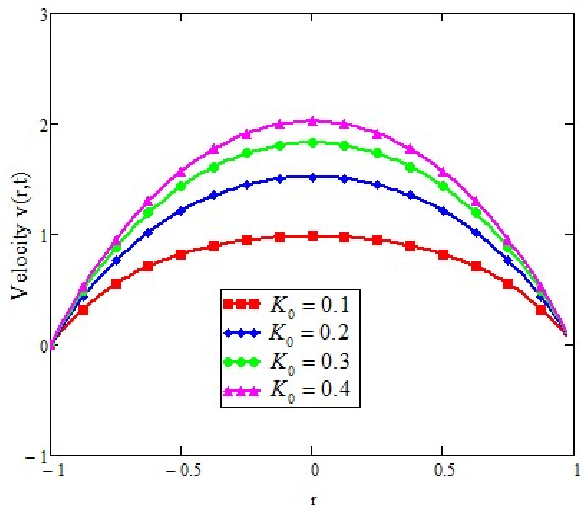

Fig. 4. Velocity profile $v(r,t)$ versus r for Oldroyd-B fluid for $t=1$, $\omega=\pi/4$ and for different values of K_0.

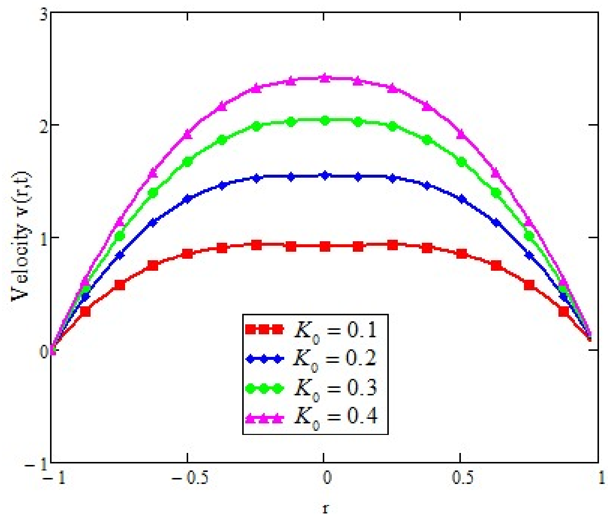

Fig. 5. Velocity profile $v(r,t)$ versus r for Burgers' fluid for $t=1$, $\omega=\pi/4$ and for different values of K_0.

Table 1. Absolute error in the numerical and analytical transient velocity $v_t(r,t)$ for $t=0.5$, $\omega=0.26$, $K_0=0.1$, $\lambda_1=0.37$, $\lambda_2=0.43$, $\lambda_3=0.59$, and $\lambda_4=0.72$.

r	Analytical transient velocity $v_t(r,t)$	Numerical transient velocity $v_t(r,t)$	Error
0	2.212307 x10^{-3}	2.212231 x10^{-3}	7.514652 x10^{-8}
0.05	2.209121 x10^{-3}	2.209046 x10^{-3}	7.470467 x10^{-8}
0.1	2.203586 x10^{-3}	2.203509 x10^{-3}	7.706446 x10^{-8}
0.15	2.19315 x10^{-3}	2.19307 x10^{-3}	7.967605 x10^{-8}
0.2	2.178049 x10^{-3}	2.177965 x10^{-3}	8.368017 x10^{-8}
0.25	2.158271 x10^{-3}	2.158183 x10^{-3}	8.800341 x10^{-8}
0.3	2.132081 x10^{-3}	2.131987 x10^{-3}	9.394519 x10^{-8}
0.35	2.099396 x10^{-3}	2.099297 x10^{-3}	9.952013 x10^{-8}
0.4	2.058958 x10^{-3}	2.058851 x10^{-3}	1.067637 x10^{-7}
0.45	2.008768 x10^{-3}	2.008654 x10^{-3}	1.139441 x10^{-7}
0.5	1.948042 x10^{-3}	1.94792 x10^{-3}	1.216925 x10^{-7}
0.55	1.8741 x10^{-3}	1.873971 x10^{-3}	1.282115 x10^{-7}
0.6	1.784366 x10^{-3}	1.784232 x10^{-3}	1.341235 x10^{-7}
0.65	1.676686 x10^{-3}	1.676549 x10^{-3}	1.377357 x10^{-7}
0.7	1.54648 x10^{-3}	1.546339 x10^{-3}	1.402362 x10^{-7}
0.75	1.390039 x10^{-3}	1.389901 x10^{-3}	1.381931 x10^{-7}
0.8	1.202816 x10^{-3}	1.202685 x10^{-3}	1.308526 x10^{-7}
0.85	9.77348 x10^{-4}	9.772318 x10^{-4}	1.162107 x10^{-7}
0.9	7.079592 x10^{-4}	7.078676 x10^{-4}	9.15698 x10^{-8}
0.95	3.863463 x10^{-4}	3.862918 x10^{-4}	5.451691 x10^{-8}
1	0	0	0

As anticipated, the drag force falls as the permeability of porous medium rises and this increases the velocity profile for all kinds of fluids. This is resemblance with the fact that the velocity profile reduces with permeability. Moreover, an examination and comparison of different types of fluids demonstrate a notable difference through Figs. 3-6. These graphs reveal that velocity profile is higher for a Burgers' fluid than those of a generalized Burgers' and an Oldroyd-B fluid, whereas the velocity profile for the Maxwell fluid is maximum. It has been seen that for the Burgers' fluid the velocity profile is monotonically increasing with respect to the parameter λ_2. However, we cannot generalize this result for selected values of λ_2, since λ_2 does not behave monotonically. Furthermore, it is observed that the velocity profile for the generalized Burgers' fluid is monotonically decreasing function of the rheological parameter λ_4. These results graphically resemble with the results found by T. Hayat, M. Khan and S. Asgar in [26] in the absence of magnetic effects.

Fig. 7 represents the trapezoidal pressure waveform influence on the fluid velocity for various fluid models. These include a generalized Burgers' fluids for which $\lambda_4 = 0.41, \lambda_3 = 0.76, \lambda_2 = 0.39, \lambda_1 = 0.2$, a Burgers' fluid for which $\lambda_4 = 0, \lambda_3 = 0.76, \lambda_2 = 0.39, \lambda_1 = 0.2$, an Oldroyd-B fluid for which $\lambda_4 = 0, \lambda_3 = 0.76, \lambda_2 = 0, \lambda_1 = 0.2$, a Maxwell fluid for which $\lambda_4 = 0, \lambda_3 = 0, \lambda_2 = 0, \lambda_1 = 0.2$ and a Newtonian fluid $\lambda_4 = 0, \lambda_3 = 0, \lambda_2 = 0, \lambda_1 = 0$. It can be seen that the Newtonian fluid and Maxwell fluid's velocity variation is trapezoidal and the time variation in the velocity for the Oldroyd-B fluid, the Burgers' fluid and the Generalized Burgers' fluid is close to the trapezoidal waveform.

Figs. 8-11 demonstrate the effects of material parameters λ_j, $j = 1,...,4$ on the generalized Burgers' fluid velocity. It can be seen from the graphs that the role of λ_1 and λ_2 on the fluid velocity is similar as well as the role of λ_3 and λ_4 is similar. The fluid velocity increases with the increase in the retardation time λ_3 whereas an opposite effect on the velocity profile of generalized Burgers' fluid is observed with the increase in the relaxation time λ_1. Moreover, the fluid velocity increases with the increase in the material parameter λ_4 and decreases with the increase in the material parameter λ_2.

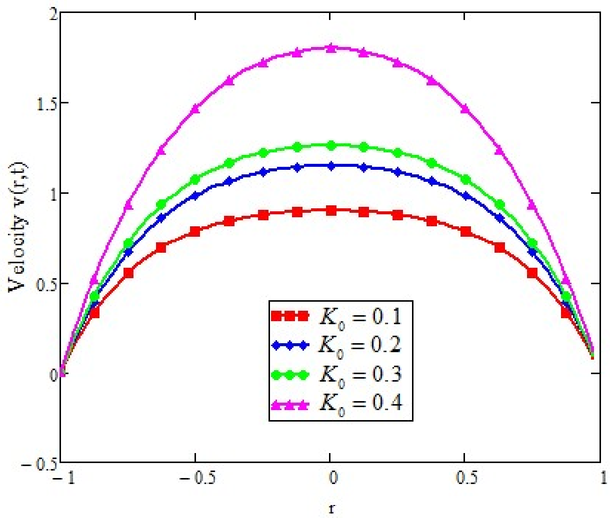

Fig. 6. Velocity profile $v(r,t)$ versus r for Maxwell fluid for $t = 1$, $\omega = \pi/4$ and for different values of K_0.

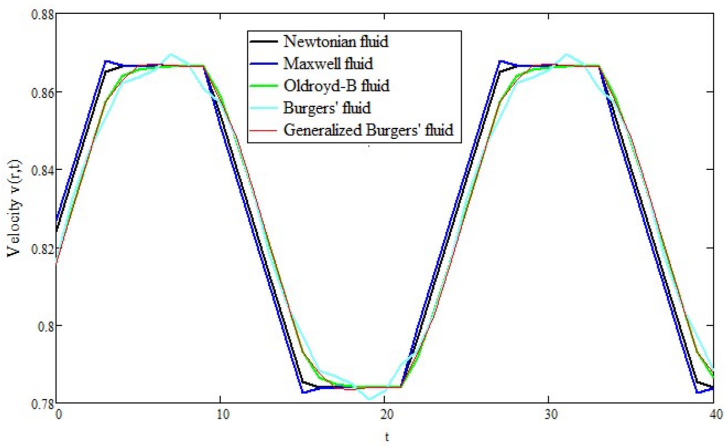

Fig. 7. Trapezoidal pressure waveform effect on velocity profile $v(r,t)$ versus t for $r = 0.56$, $\omega = \pi/12$, $K_0 = 0.25$ and different fluids.

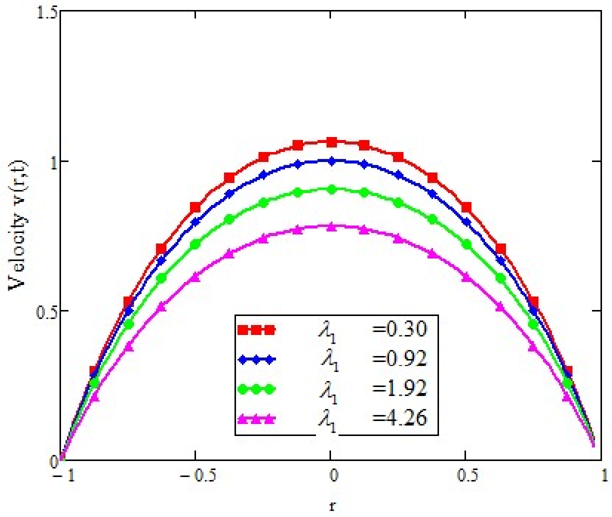

Fig. 8. Velocity profile $v(r,t)$ versus r for $t=10$, $\omega=\pi/3$, $K_0=0.25, \lambda_2=1.9, \lambda_3=0.81, \lambda_4=0.66$, for different val. of λ_1.

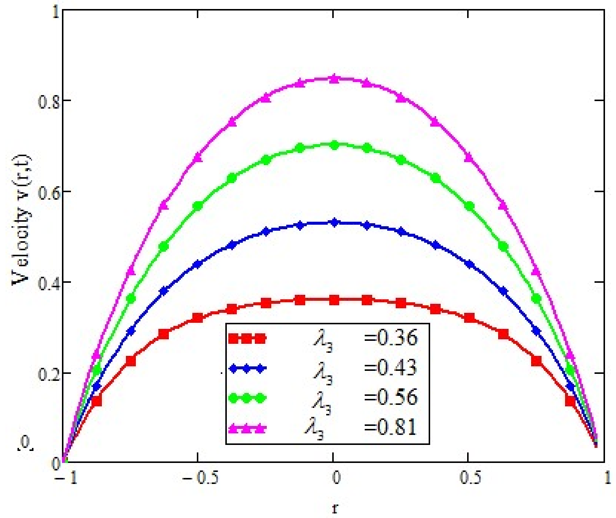

Fig. 9. Velocity profile $v(r,t)$ versus r for $t=10$, $\omega=\pi/3$, $K_0=0.25$, $\lambda_1=2.6$, $\lambda_2=1.9$, $\lambda_4=0.66$ and for different values of λ_3.

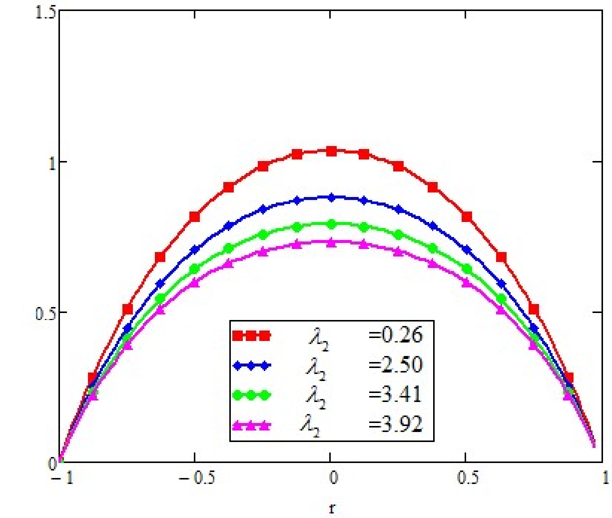

Fig. 10. Velocity profile $v(r,t)$ versus r for $t=10$, $\omega=\pi/3$, $K_0=0.25$, $\lambda_1=1.63$, $\lambda_3=0.81$, $\lambda_4=0.66$ and for different values of λ_2.

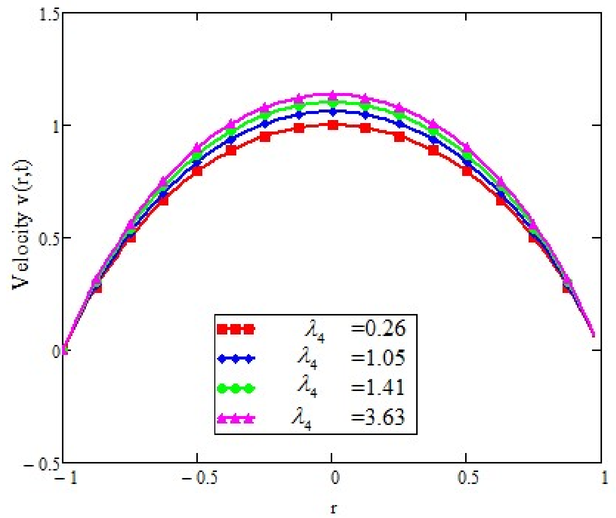

Fig. 11. Velocity profile $v(r,t)$ versus r for $t=10$, $\omega=\pi/3$, $\lambda_1=1.63$, $\lambda_2=0.72$, $\lambda_3=0.81$ and for different values of λ_4.

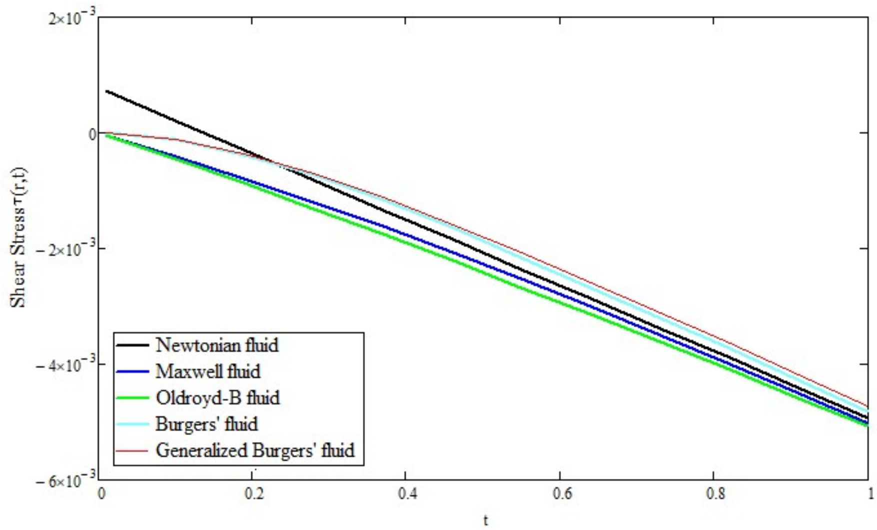

Fig. 12. Trapezoidal pressure waveform effect on velocity profile $\tau_{rz}(r,t)$ versus t for $r=0.56$, $\omega=\pi/12$, $K_0=0.25$, $\mu=0.3$ and different fluids.

Fig. 12 represents the trapezoidal pressure waveform influence on the fluid shear stress for various fluid models. These include a generalized Burgers' fluids for which $\lambda_4 = 0.97, \lambda_3 = 0.76, \lambda_2 = 0.1, \lambda_1 = 0.6$, a Burgers' fluid for which $\lambda_4 = 0, \lambda_3 = 0.76$, $\lambda_2 = 0.1, \lambda_1 = 0.6$, an Oldroyd-B fluid for which $\lambda_4 = 0, \lambda_3 = 0.76, \lambda_2 = 0, \lambda_1 = 0.6$ a Maxwell fluid for which $\lambda_4 = 0, \lambda_3 = 0$, $\lambda_2 = 0, \lambda_1 = 0.6$ and a Newtonian fluid $\lambda_4 = 0, \lambda_3 = 0, \lambda_2 = 0, \lambda_1 = 0$. The shear stress is linear for the Newtonian fluid, the Maxwell fluid and the Oldroyd-B fluid is linear and is curvilinear for the Generalized Burgers' fluid and the Burgers' fluid. The shear stress profile for the Generalized Burgers' fluid and the Burgers' fluid is close each other and is higher as compare to the Oldroyd-B fluid, the Maxwell fluid and the Newtonian fluid. Fig. 13 represents the effect of dynamic viscosity μ on shear stress τ_{rz} for generalized Burgers' fluid for which $\lambda_4 = 0.96, \lambda_3 = 0.81, \lambda_2 = 0.76, \lambda_1 = 0.66$. It has been seen that shear stress decreases with the increase in the dynamic viscosity.

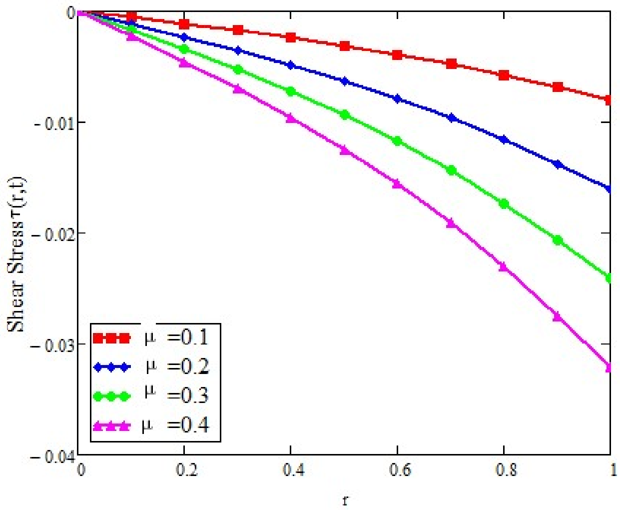

Fig. 13. Velocity profile $v(r,t)$ versus r for generalized Burgers' fluid for $t = 10$, $\omega = \pi / 4$, $K_0 = 0.3$ and for different values of μ.

5. Conclusions

The exact analytical solution for the Generalized Burgers' fluid flow through a cylindrical microchannel in the presence of the trapezoidal pressure waveform is derived for velocity profiles with the help of similarity arguments and finite Hankel transforms. A Semi-analytic solution for motion is developed with the help of Stehfest's method to verify the validity of the obtained solution. The following is a summary of the main findings in the paper.
- As anticipated, the drag force falls as the permeability of porous medium rises and this increases the velocity profile for all kinds of fluids (a generalized Burgers' fluids, a Burgers' fluid, a Maxwell fluid and an Oldroyd-B fluid). This is resemblance with the fact that the velocity profile reduces with permeability.
- The velocity time variation of the Newtonian fluid is trapezoidal, which is close to the Generalized Burgers' fluid and the Oldroyd-B fluid, whereas the velocity time variation behavior for the Burgers' and the Maxwell fluid is different.
- The material constants λ_i, $i = 1,...,4$ have significant effects on the fluid velocity.

Conflict of Interest

The author(s) declared no potential conflicts of interest with respect to the research, authorship and publication of this article.

Funding

The author(s) received no financial support for the research, authorship and publication of this article.

References

[1] Tan, W., Xian, F. and Wei, L., An exact solution of unsteady Couette flow of generalized second grade fluid. *Chinese Science Bulletin*, 47(21), 2002, 1783-1785.
[2] Qi, H. and Jin, H., Unsteady rotating flows of a viscoelastic fluid with the fractional Maxwell model between coaxial cylinders. *Acta Mechanica Sinica*, 22(4), 2006, 301-305.
[3] Hayat, T., Nadeem, S. and Asghar, S., Periodic unidirectional flows of a viscoelastic fluid with the fractional Maxwell model. *Applied Mathematics and Computation*, 151(1), 2004, 153-161.
[4] Khan, M., Maqbool, K. and Hayat, T., Influence of Hall current on the flows of a generalized Oldroyd-B fluid in a porous

space. *Acta Mechanica*, 184(1-4), 2006, 1-13.
[5] Huang, J., He, G. and Liu, C., Analysis of general second-order fluid flow in double cylinder rheometer. *Science in China Series A: Mathematics*, 40(2), 1997, 183-190.
[6] Xu, M. and Tan, W., Theoretical analysis of the velocity field, stress field and vortex sheet of generalized second order fluid with fractional anomalous diffusion. *Science in China Series A: Mathematics*, 44(11), 2001, 1387-1399.
[7] Jyothi, K.L., Devaki, P. and Sreenadh, S., Pulsatile flow of a Jeffrey fluid in a circular tube having internal porous lining. *International Journal of Mathematical Archive*, 4(5), 2013.
[8] Ghosh, A.K. and Sana, P., On hydromagnetic channel flow of an Oldroyd-B fluid induced by rectified sine pulses. *Computational & Applied Mathematics*, 28(3), 2009, 365-395.
[9] Elshehawey, E.F., Eldabe, N.T., Elghazy, E.M. and Ebaid, A., Peristaltic transport in an asymmetric channel through a porous medium. *Applied Mathematics and Computation*, 182(1), 2006, 140-150.
[10] Lin, F.H., Liu, C. and Zhang, P., On hydrodynamics of viscoelastic fluids. *Communications on Pure and Applied Mathematics*, 58(11), 2005, 1437-1471.
[11] Thurston, G.B., Theory of oscillation of a viscoelastic medium between parallel planes. *Journal of Applied Physics*, 30(12), 1959, 1855-1860.
[12] Thurston, G.B., Theory of oscillation of a viscoelastic fluid in a circular tube. *The Journal of the Acoustical Society of America*, 32(2), 1960, 210-213.
[13] Jones, J.R. and Walters, T.S., Flow of elastico-viscous liquids in channels under the influence of a periodic pressure gradient, part 1. *Rheologica Acta*, 6(3), 1967, 240-245.
[14] Jones, J.R. and Walters, T.S., Flow of elastico-viscous liquids in channels under the influence of a periodic pressure gradient part II. *Rheologica Acta*, 6(4), 1967, 330-338.
[15] Rahaman, K.D. and Ramkissoon, H., Unsteady axial viscoelastic pipe flows. *Journal of Non-newtonian Fluid Mechanics*, 57(1), 1995, 27-38.
[16] Walitza, E., Maisch, E., Chmiel, H. and Anadere, I., Experimental and numerical analysis of oscillatory tube flow of viscoelastic fluids represented at the example of human blood. *Rheologica Acta*, 18(1), 1979, 116-121.
[17] Manos, T., Marinakis, G. and Tsangaris, S., Oscillating viscoelastic flow in a curved duct—exact analytical and numerical solution. *Journal of Non-newtonian Fluid Mechanics*, 135(1), 2006, 8-15.
[18] Khan, M., Anjum, A., Fetecau, C. and Qi, H., Exact solutions for some oscillating motions of a fractional Burgers' fluid. *Mathematical and Computer Modelling*, 51(5-6), 2010, 682-692.
[19] Zheng, L., Li, C., Zhang, X. and Gao, Y., Exact solutions for the unsteady rotating flows of a generalized Maxwell fluid with oscillating pressure gradient between coaxial cylinders. *Computers & Mathematics with Applications*, 62(3), 2011, 1105-1115.
[20] Ruckmongathan, T.N., Techniques for reducing the hardware complexity and the power consumption of drive electronics, 2006.
[21] Hayat, T., Khan, S. B., Khan, M., Exact solution for rotating flows of a generalized Burgers's fluid in a porous space. *Applied Mathematical Modelling*, 32, 2008, 749-760.
[22] Hayat, T., Khan, M. and Asghar, S., On the MHD flow of fractional generalized Burgers' fluid with modified Darcy's law. *Acta Mechanica Sinica*, 23(3), 2007, pp.257-261.
[23] Khuzhayorov, B., Auriault, J.L. and Royer, P., Derivation of macroscopic filtration law for transient linear viscoelastic fluid flow in porous media. *International Journal of Engineering Science*, 38(5), 2000, 487-504.
[24] Dettman, J.W., *Introduction to linear algebra and differential equations*. Courier Corporation, 1986.
[25] Stehfest, H., Algorithm 368: Numerical inversion of Laplace transforms [D5]. *Communications of the ACM*, 13(1), 1970, 47-49.
[26] Stehfest, H., Remark on algorithm 368: Numerical inversion of Laplace transforms. *Communications of the ACM*, 13(10), 1970, 624.
[27] Hayat, T., Khan, M. and Asghar, S., On the MHD flow of fractional generalized Burgers' fluid with modified Darcy's law. *Acta Mechanica Sinica*, 23(3), 2007, 257-261.
[28] Gaver Jr, D.P., Observing stochastic processes, and approximate transform inversion. *Operations Research*, 14(3), 1996, 444-459.
[29] Davies, B., *Integral transforms and their applications* (Vol. 41). Springer Science & Business Media, 2012.

Appendix

Derivation of Stehfest's Algorithm

The method originates from Graver [28], where he considered sampling a function $f(t)$ with respect to the family of probability density functions

$$\chi_m(c,t) = \frac{c(2m)!}{m!(m-1)!}[1-\exp(-ct)]^m \exp(-mct) \quad c > 0. \tag{A1}$$

These functions are used to define the expectation of the function $f(t)$ as

$$\tilde{f}_m = \int_0^\infty f(t)\chi_m(c,t)dt \tag{A2}$$

Using binomial expansion for $[1-\exp(-ct)]^K$ and Eqs. (A1), (A2) we can write $\tilde{f}_K$ in equivalent form

$$\tilde{f}_m = \frac{c(2m)!}{m!(m-1)!}\sum_{i=1}^{m}(-1)^i\binom{m}{i}\bar{f}((m+i)c) \tag{A3}$$

where $\bar{f}(q) = \int_0^\infty f(t)e^{-qt}dt$. Graver [28] also proved the asymptotic expansion

$$\tilde{f}_m \approx f(\frac{\ln 2}{c}) + \frac{\beta_1}{m} + \frac{\beta_2^2}{m^2} + \cdots \tag{A4}$$

which illustrates the convergence nature of $\tilde{f}_m$ to the Laplace inverse function value $f(\ln 2/c)$ as $m \to \infty$. Later Stehfest [25] improved the Graver work for the approximation to $f(\ln 2/c)$ as

$$f\left(\frac{\ln 2}{c}\right) = \sum_{m=1}^{\frac{M}{2}}\alpha_m\tilde{f}_m + \mathcal{O}\left(1/M^{M/2}\right) \tag{A5}$$

where coefficients α_K satisfy

$$\sum_{m=1}^{\frac{M}{2}}\alpha_m\frac{1}{\left(1+M/2-m\right)^j} = \delta_{j0}, \quad j = 0,1,...M/2-1 \tag{A6}$$

and is given by

$$\alpha_m = \frac{(-1)^{m-1}m(1+M/2-m)^{M/2-1}}{(M/2)!}\binom{M/2}{m} \tag{A7}$$

Finally, the inversion formula (47) and (48) can be recovered by substituting these results in (A5) and replacing $f(t) = v_t(r,t)$ and $\bar{f}(t) = \bar{v}_t(r,t)$. Further details on the derivation can be seen in [25, 28, 29]